ResearchGate

See discussions, stats, and author profiles for this publication at: https://www.researchgate.net/publication/268512336

Visible/Infrared Dissociation of NO3: Roaming in the Dark or Roaming on the Ground?

ARTICLE *in* THE JOURNAL OF PHYSICAL CHEMISTRY A · JULY 2015

Impact Factor: 2.69 · DOI: 10.1021/jp509902d

CITATIONS
2

READS
58

7 AUTHORS, INCLUDING:

Ravin Fernando
University of Missouri
8 PUBLICATIONS **22** CITATIONS
SEE PROFILE

Arghya Dey
Radboud University Nijmegen
17 PUBLICATIONS **59** CITATIONS
SEE PROFILE

Bina Fu
Chinese Academy of Sciences
39 PUBLICATIONS **613** CITATIONS
SEE PROFILE

Joel M Bowman
Emory University
542 PUBLICATIONS **15,124** CITATIONS
SEE PROFILE

Available from: Ravin Fernando
Retrieved on: 27 January 2016

THE JOURNAL OF PHYSICAL CHEMISTRY A

Article

pubs.acs.org/JPCA

Visible/Infrared Dissociation of NO_3: Roaming in the Dark or Roaming on the Ground?

Ravin Fernando,[†] Arghya Dey,[†] Bernadette M. Broderick,[†] Bina Fu,[‡] Zahra Homayoon,[§] Joel M. Bowman,[§] and Arthur G. Suits*[,†]

[†]Department of Chemistry, Wayne State University, 5101 Cass Avenue, Detroit, Michigan 48202, United States

[‡]State Key Laboratory of Molecular Reaction Dynamics, Dalian Institute of Chemical Physics, Chinese Academy of Sciences, 457 Zhongshan Road, Dalian 116023, China

[§]Department of Chemistry and Cherry L. Emerson Center for Scientific Computation, Emory University, 201 Dowman Drive, Atlanta, Georgia 30322, United States

ABSTRACT: We present a DC slice imaging study of roaming dynamics in the photodissociation of the nitrate radical, NO_3, contrasting pure visible excitation with a combination of visible and CO_2 laser excitation at 10.6 μm. Images of specific rotational levels of NO are seen to reflect dissociation on the ground and first excited electronic states, as reported in previous work. The branching is obtained for specific rotational levels by comparison to quasiclassical trajectory calculations of the dynamics on these two surfaces. The results for the visible dissociation are found to be very similar to the combination of visible and infrared, raising questions about the nature of the coupling of these surfaces, the extent to which roaming takes place on both, and how the final product branching is determined.

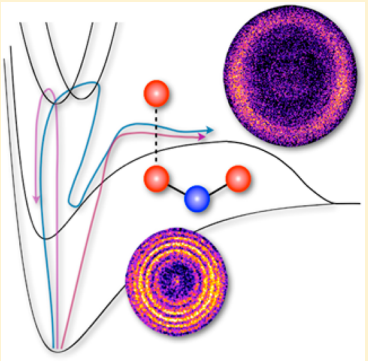

INTRODUCTION

The nitrate radical, NO_3, is an extraordinary molecule that has fascinated and challenged chemists for many years.[1,2] It possesses several low-lying electronically excited states showing complex vibronic interactions accessible via visible excitation.[3−6] Its photochemistry is also quite unusual, with two dissociation channels, NO + O_2 and NO_2 + O, showing nearly the same energy threshold and accessible in the visible,[7−9] giving it an important role in the atmosphere.[10] In hindsight, the close connection between these two reaction channels may be seen as a portent of the recent recognition of the key role of roaming dynamics in this system.[11−13] Roaming is a reaction mechanism in which the molecule undergoes near-dissociation to products, following which reorientation gives access to a distinct intramolecular reactive pathway.[14] It is now recognized as a ubiquitous but long-overlooked mechanism by which molecules decompose.[15−17]

Roaming in the case of NO_3 is quite unusual, however. Key features of the relevant potential energy surfaces (PESs) are shown in Figure 1 to guide this discussion. In recent imaging studies, Grubb et al.[11] found that rotationally selected NO translational energy distributions fell into two distinct groups associated with distinct O_2 vibrational distributions. The low rotational levels were formed with vibrationally excited O_2, while higher rotational levels were associated with vibrationally colder O_2. On the basis of a careful search of the stationary points and the intersections among the relevant PESs, Morokuma and co-workers[18] suggested the following picture

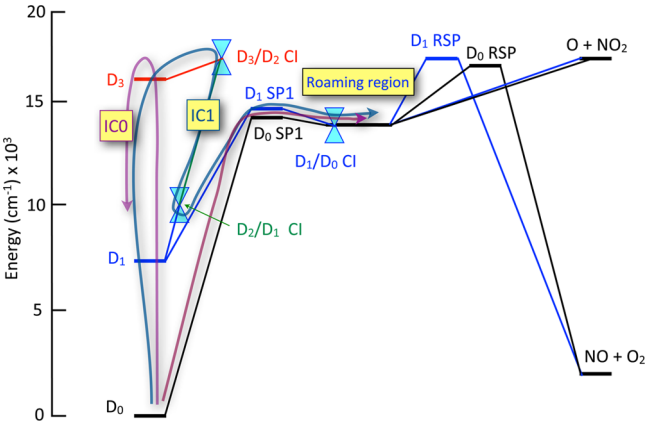

Figure 1. Key points on the four lowest adiabatic potential surfaces of NO_3 from Morokuma and co-workers (ref 18). D_0 and D_1 SP1 are saddle points separating the well from the roaming region on the two surfaces, and D_0 and D_1 RSP are RSPs leading to NO + O_2. Minimum-energy CIs are also shown. IC0 schematically portrays direct internal conversion from D_3 to D_0, while IC1 represents the IC pathway that follows the succession of CIs shown.

Special Issue: 100 Years of Combustion Kinetics at Argonne: A Festschrift for Lawrence B. Harding, Joe V. Michael, and Albert F. Wagner

Received: September 30, 2014
Revised: November 15, 2014

 © XXXX American Chemical Society dx.doi.org/10.1021/jp509902d | J. Phys. Chem. A XXXX, XXX, XXX−XXX

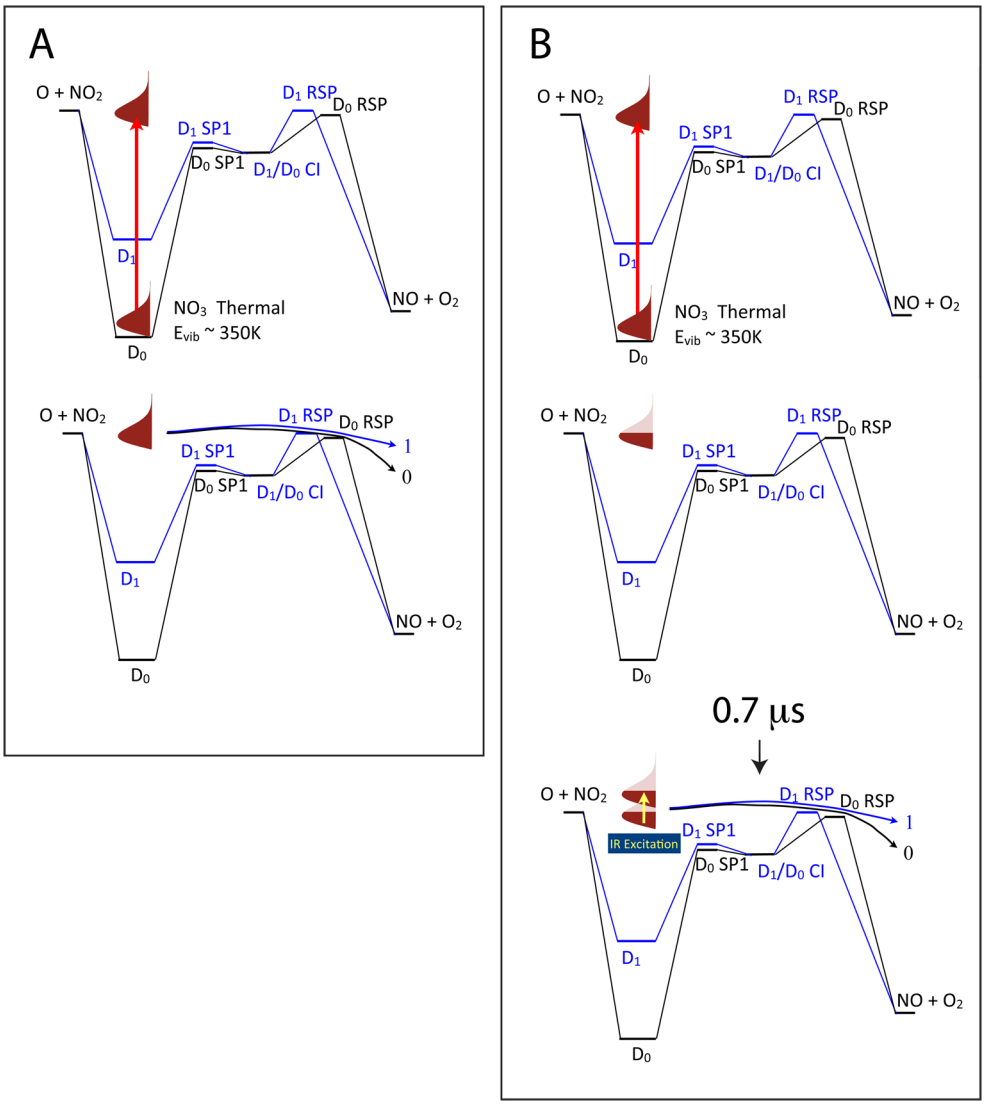

Figure 2. Schematic of the experimental approach. (A) Visible excitation of thermal ground state NO_3 leads to prompt dissociation for a subset of the initial population via channels D_1 and D_0. (B) Visible excitation is followed by a 0.7 μs delay, creating a population of NO_3 just below the dissociation threshold. The CO_2 laser pulse then promotes these molecules over the dissociation threshold where they again appear as dissociation products via channels D_1 and D_0.

of its dissociation dynamics. After optical excitation to the D_3 state (the lower member of the Jahn−Teller distorted E′ pair), the system relaxes via the D_3/D_2 and D_2/D_1 conical intersections (CIs) to arrive on the dark D_1 state. They argued that the vibrationally colder O_2 product arises from roaming dynamics on D_1 (via the D_1 roaming saddle point (RSP) given in Figure 1), while the vibrationally excited O_2 arises via dissociation from the ground electronic state via the D_0 RSP. Strong support for this assignment was seen in the λ doublet propensities, which were found to be opposite and perhaps near-limiting for the two distributions,[12,19] as well as in subsequent quasiclassical trajectory (QCT) calculations on separate, uncoupled D_0 and D_1 potential surfaces.[20] These remarkable results prompt several questions: What is the branching for dissociation on these two surfaces? What determines this branching? Does roaming take place exclusively on the dark state or on the ground state, with branching upon exit or on both? Is the branching determined at the intersection between the D_1 and D_0 surfaces in the course of electronic relaxation or possibly from D_0 up to D_1 after an initial relaxation from the bright D_3 state to D_0? To begin addressing these questions, we here combine state-selected DC slice imaging of the NO product following visible or a combination of visible and infrared excitation from a CO_2 laser, along with additional QCT calculations.

METHODS

Experimental Section. N_2O_5 was used as the precursor for NO_3. The N_2O_5 product was placed in an ice bath, and He (800 Torr) was sent through to prepare the gas mixture. NO_3 was produced by pyrolysis of N_2O_5 at 350 °C using a resistively heated extension tube on a solenoid operated pulsed valve. The NO_3 molecular beam was skimmed and then intersected with three laser beams, 622.9 nm, 226 nm, and 10.6 μm. The 622.9 nm beam was generated from the fundamental output of a pulsed dye laser (Sirah, DCM in ethanol) pumped by the second harmonic of a Nd:YAG laser. The 226 nm beam was generated by mixing the third harmonic of an injection-seeded Nd:YAG laser with the fundamental output of a pulsed dye laser (Sirah, DCM in ethanol) pumped by the second harmonic

dx.doi.org/10.1021/jp509902d | J. Phys. Chem. A XXXX, XXX, XXX−XXX

of the same Nd:YAG laser. The IR beam, 10.6 μm, was produced by a grating-tuned TEA-CO_2 laser (GAM laser). The power of the 622.9 nm beam was ~3.0 mJ/pulse, that of the 226 nm beam was ~0.05 mJ/pulse, and the IR was ~100 mJ/pulse. The 622.9 nm beam was ~2 mm upstream relative to the 226 nm beam for the two-color photolysis experiments. The 226 nm beam and IR beams were counterpropagating. The 622.9 nm was 700 ns prior to the 226 nm, and the IR beam was 250 ns prior to the 226 nm beam. The ions originating from the beams were accelerated through a time-of-flight tube toward a 120 mm microchannel plate detector coupled with a P-47 phosphor screen. A USB CCD camera was used to capture the ion images, and the acquisition was done using our own NuACQ program. The acquired images were used to obtain the total translational energy distributions. The NO probe wavelengths were monitored using a wavemeter and assigned using the LIFBASE program[21] to well-isolated levels of the indicated rotational branches.

Computational Section. The ab initio global PESs of the ground (D_0) and the first excited (D_1) electronic states for photodissociation of NO_3 were calculated based on roughly 90 000 MS-CAS(17e,13o)PT2/aug-cc-pVTZ calculations of electronic energies,[18] using the permutationally invariant polynomial fitting method.[26,27] Standard QCT calculations were performed on the fitted PESs to get detailed dynamics information on NO + O_2 products. Roughly 400 000 trajectories were run initiated from the RSPs of D_0 and D_1 with initial conditions generated using microcanonical random sampling of the initial kinetic energy and with the constraint of zero total angular momentum, respectively. The trajectories were propagated with the time step of 0.12 fs using the velocity Verlet integrator. Most of the trajectories were propagated for a maximum of 20 000 time steps (~2 ps), indicating fairly prompt, direct dynamics from D_0 and D_1 RSPs. The trajectories were terminated when one of the internuclear distances became larger than 14 bohr. For those trajectories resulting in NO + O_2 products, the ZPE (zero-point energy) constrained analysis is employed for those trajectories in which NO and O_2 products have at least the corresponding ZPEs.[22] Trajectories that violate the ZPE were discarded. Furthermore, additional trajectories were initiated on D_1 to investigate the energy gaps between the D_1 and D_0 PESs. The ground vibronic state Wigner distribution is typically used to select the initial conditions on the excited-state potential, here D_1.

Densities of states of global minima of D_0 and D_1 (DO-GM and D1-GM) are calculated using the semiclassical approach. Harmonic frequencies and ZPEs of DO-GM and D1-GM are calculated using the D_0 and D_1 PESs, respectively.[19] Results are given in the next section.

RESULTS AND DISCUSSION

Ideally, to probe the question whether roaming takes place exclusively on the excited state or the ground state, one might contrast dissociation following electronic excitation with that arising from infrared multiphoton excitation. Unfortunately, NO_3 has no infrared-active bands that overlap the CO_2 laser lines; therefore, direct CO_2 laser excitation is not readily achieved. However, several of the unusual properties of NO_3 allow us to begin an investigation along these lines using state-selected DC slice imaging as in the earlier experiments but contrasting pure electronic excitation with a *combination* of electronic and infrared excitation. This approach is summarized in Figure 2. NO_3 is produced in a molecular beam by flash pyrolysis of N_2O_5 at ~350 °C, yielding a beam that is rotationally cold but with a broad vibrational distribution. Visible excitation at 623 nm excites the molecules initially to D_3. As shown by Davis et al., this excitation energy is below the dissociation threshold at 0 K, but even at 300 K, the quantum yield for the NO + O_2 channel at 623 nm is ~15% (with the remaining 85% decaying by fluorescence).[9] Prompt dissociation (i.e., within the 10 ns probe time) of that "hot band" population that exceeds the dissociation threshold gives rise to NO + O_2, which is probed using DC slice imaging[23] of state-selected NO molecules (Figure 2A), although a large fraction of the electronically excited molecules do not have sufficient energy to dissociate. This allows us to study the dissociation just at threshold. In a separate experiment, schematically illustrated in Figure 2B, NO_3 is optically excited 1−2 mm upstream of the interaction region. The prompt dissociation is allowed to occur, and then 0.7 μs later, after electronic relaxation, an intense IR laser pulse at 10.6 μm further excites the undissociated molecules over the dissociation threshold. This delay is chosen to maximize the signal when the electronic excitation is moved upstream as far as is practical. Again, state-resolved slice imaging of the NO product is performed. This allows us to distinguish any dissociation that occurs during the initial electronic relaxation from the long-time behavior of the system. These results are then compared to QCT calculations on the uncoupled surfaces in order to estimate the branching for dissociation on D_0 or D_1.

We performed the two distinct experiments described above, and for each rotational level, we obtained images on P or R branches and on Q branches following the strategy of North and co-workers.[12] Given the large λ doublet propensities seen and the distinct behavior for dissociation on the two surfaces, this is necessary both to aid in assigning clearly the D_0 and D_1 contributions to the dissociation and to determine the branching. The images for visible and visible/IR dissociation are shown in Figure 3 for the indicated NO rotational level and the rotational branch of NO used in the probe. As may readily be seen, there are profound differences for Q branch detection as opposed to detection via P,R branches, and this is consistent with the North results. The Q branch probe appears to favor the higher rotational levels that were associated with the D_1 dissociation by Morokuma,[18,24] while the P,R probe appears dominant for the lower rotational levels that show clear vibrational structure and high vibrational excitation for the O_2 co-product in some cases. This sharply structured low-J component was assigned to dissociation on the ground electronic state, and this was confirmed in the QCT calculations.[20]

We obtained the total translational energy distributions ($P(E)$'s) from the images, and these are given in Figure 3 as well. Although we see distinct differences for each probed rotational level and detection pathway, the results for prompt dissociation with purely electronic excitation shown on the right of Figure 3 show little difference when compared to dissociation with a combination of visible and infrared after a 0.7 μs delay. Before discussing the implications of this observation, we first obtain an estimate of the branching between the two dissociation paths based on the measured distributions. Our strategy here is first to create composite translational energy distributions by weighting the distributions in Figure 3 using the appropriate line strength factors[25] and then fitting the composite distribution with separate D_0 and D_1 components obtained from the QCT calculations. The results

dx.doi.org/10.1021/jp509902d | J. Phys. Chem. A XXXX, XXX, XXX−XXX

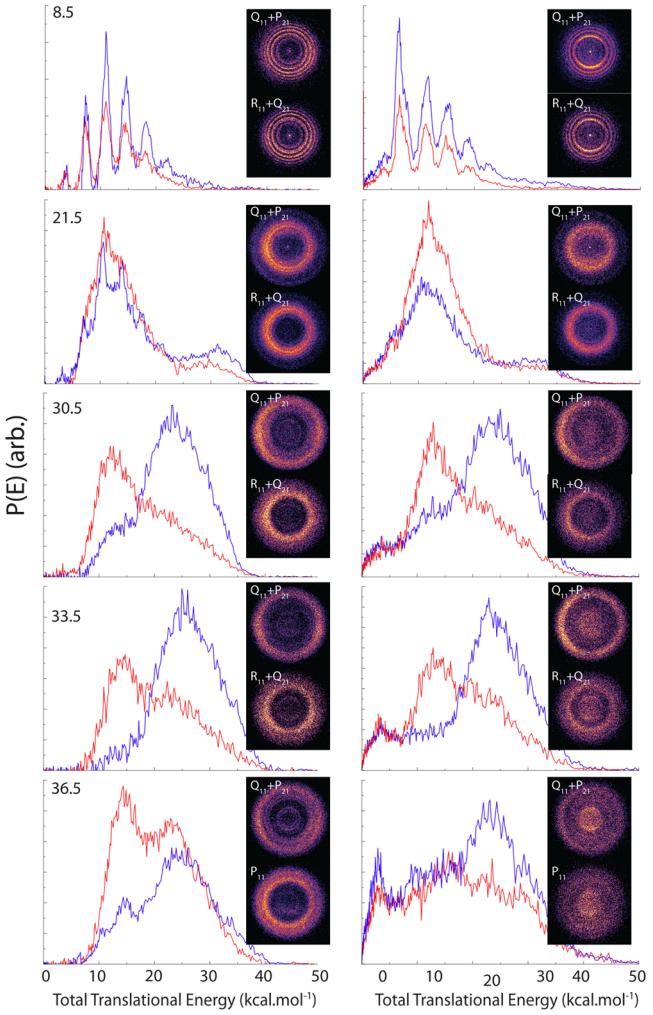

Figure 3. NO(v=0, J) DC slice images and total translational energy distributions for visible + IR dissociation (left) or pure visible dissociation (right) for the indicated rotational level and probe transition. Curves in blue are for Q main branch detection, and those in red are for R or P main branch detection. The visible data show a minor contribution from the background from dissociation by the probe laser at lower translational energies that has not been subtracted.

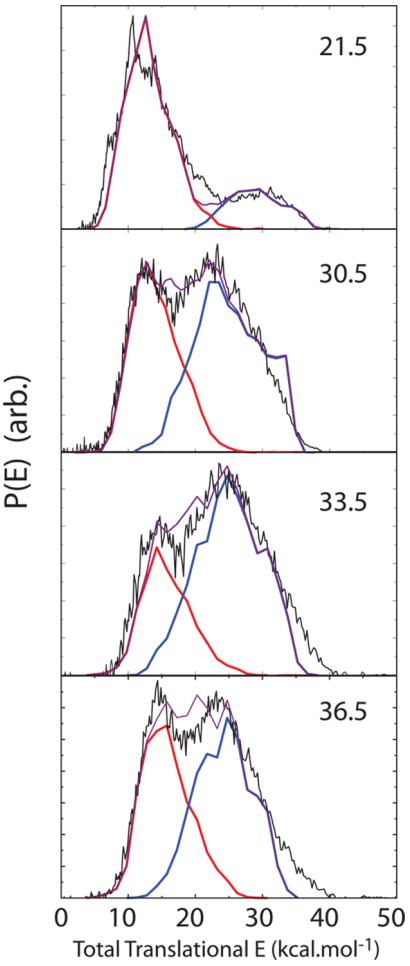

Figure 4. Composite translational energy distributions for indicated NO rotational levels obtained by weighting the Q and R,P probe data from Figure 2 by the appropriate line strength factors and then summing them. The composite distributions were then fitted using the separate D_0 and D_1 contributions obtained from the QCT calculations (red and blue curves, respectively). The translational energy for the D_0 components for J = 21.5 and 30.5 was scaled by 80 and 95%, respectively, to obtain accurate fits; otherwise, only the amplitudes were adjusted.

are shown in Figure 4. The agreement is generally satisfactory. The relative yields for D_0/D_1 from the fits were found to be 0.92, 0.49, 0.31, and 0.44 for rotational levels 21.5, 30.5, 33.5, and 36.5, respectively. Lower rotational levels are associated exclusively with D_0. This state-dependent branching was then used, with linear interpolation over the rotational distributions given by Wittig and co-workers,[8] to obtain a final branching for dissociation of 6:1 D_0/D_1. This analysis neglects the minor ν = 1 contribution, which has been found to favor D_0 dissociation,[13] as well as rotational levels above J = 40.5, which were not reported by Wittig but are likely to represent a minor contribution. This is largely consistent with the determination of North and co-workers[19] and with the overall translational energy distributions reported by Davis and Lee,[7] although we note that even in our raw images, we see a greater contribution of the slow component than was seen by North and co-workers. It may be that our excitation, which is at somewhat lower energy than in previous photodissociation studies and just above the dissociation threshold, actually gives rise to some greater discrimination between the energies of the RSPs on D_0 and D_1. We plan further experiments to address this question.

We now turn to a consideration of the electronic relaxation and dissociation dynamics. The main possibilities, highlighted in Figure 1, include initial excitation to the D_3 bright state followed by internal conversion (IC1) through D_2 and D_1 to D_0 via the CIs that were found by Morokuma and co-workers.[20] This pathway is shown as "IC1" in Figure 1. The branching for dissociation along D_1 or D_0 that we measure may then reflect the branching at the D_1/D_0 CI as it is encountered during the relaxation. This is the pathway implicit in the treatment of Grubb et al.[12] Alternatively, excitation to the bright state may be followed by IC to the ground state directly from D_3, shown as "IC0" on Figure 1. The distinction here is that we recognize that D_3 and D_0 are directly vibronically coupled;[4] therefore, the ground state need not be accessed primarily via D_1 in the roaming region. In this scenario, after IC to D_0, the system may proceed to the roaming region and then "roam upstairs" via the D_0/D_1 CI, which is located in the roaming region. From there, it may roam on D_1 or simply dissociate. If the energy is above

dx.doi.org/10.1021/jp509902d | J. Phys. Chem. A XXXX, XXX, XXX−XXX

the O atom loss threshold, decay via that path is strongly preferred both for D_1 and D_0, based on both experiment[7] and the trajectory calculations.[20]

One significant feature of NO_3 photophysics impacts this discussion. In the visible region, it is an example of the "Douglas effect," with an anomalously long fluorescence lifetime following excitation to the D_3 state.[26] This is ascribed to mixing of the bright D_3 state with the dense manifold of D_0 and possibly D_1 levels in which it is embedded.[27] Its "long-time limit" thus includes an admixture of the D_3 state with D_0. Indeed, at 0.7 μs, we may be in a fully statistical mixture of the accessible electronic states. This is supported by our calculations of the harmonic vibrational density of states using. At 16 200 cm^{-1}, which is roughly the D_3 origin, we obtain state densities of 133 and 17 per cm^{-1}, or a ratio of 8.4:1, which is reasonably close to the experimental branching estimate of 6:1. This density of states ratio would be the RRKM statistical approximation for the experimental branching ratio if the roaming bottlenecks N(E)'s on D_1 and D_0 are the same. Clearly, they are not identical, and if the slightly higher energy of RS1 relative to RS0 is a good indicator of the N(E)'s, then indeed the branching would be slightly less than 8.4:1 and thus closer to experiment. As suggestive as this is, one should take this analysis with a great deal of caution.

Taking all of these points into consideration, we believe that the evidence supports the second alternative relaxation pathway mentioned above, that is, direct IC from the bright state to D_0, with D_1 subsequently accessed from the ground state, probably via mixing in the roaming region where these surfaces are strongly coupled, as shown in Figure 5. The points in support

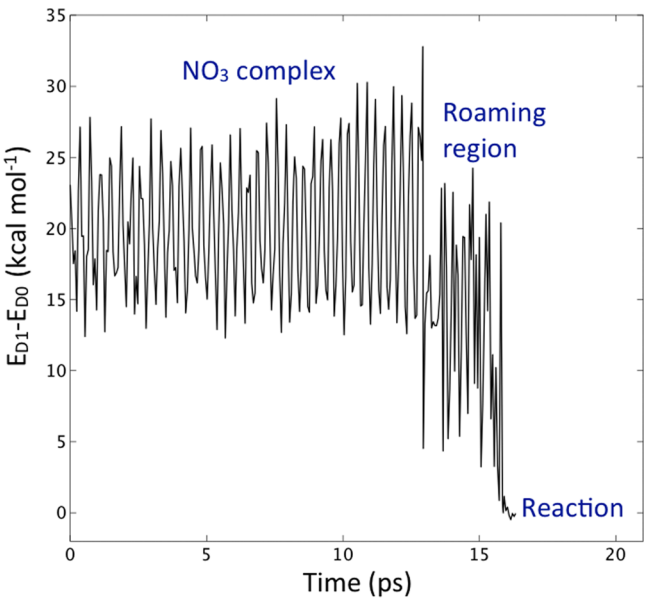

Figure 5. Energy splitting between D_0 and D_1 during the course of a typical trajectory. This trajectory was initiated at the D_0 GM with microcanonical sampling of the initial momenta for total angular momentum $J = 0$.

of this view are as follows: The D_3 and D_0 surfaces possess strong vibronic coupling, directly impacting both the ground-state vibrational level structure and the bright-state fluorescence lifetimes, while that between the bright state and D_1 is very weak.[5] Moreover, the fluorescence lifetimes suggest a dilution of the bright state that can only be accounted for by the ground-state density of states.[27,28] The fact that our translational energy distributions are essentially identical whether we use electronic excitation with a probe on a 10 ns time scale or one coupled with IR excitation 0.7 μs later suggests that this relaxation is complete on the 10 ns time scale.

One other suggestive point from Morokuma's calculations is that the D_3/D_2 minimum-energy CI is at 200.8 kJ/mol, which is nominally above the energy window that gives O_2 + NO and in the region where the branching to NO_2 + O is dominant. It is interesting to speculate whether this is a coincidence or not; perhaps the branching to the atomic elimination channel grows quickly because of the direct access to D_1 that arises via the succession of CIs just as that channel is opened. The QC trajectories from the D_1 global minimum branched more to the atomic elimination than did those on D_0 at the same total energy, providing some support for this picture.[20] In any case, efficient access to D_1 from D_2 seems implausible under our experimental conditions if this location of the D_2/D_1 minimum-energy CI is correct. Although the notion of traversing the D_0/D_1 CI in the upward direction[29] ("upfunneling") might seem less likely as flux is typically directed away from a CI upon approach from below, because the surfaces are relatively flat and parallel in this region, this view may not be relevant. This aspect of the dynamics is highlighted in the trajectory shown in Figure 5. This plot shows the energy splitting between the D_1 surface and the D_0 surface during the course of a typical trajectory. In the complex region, the D_1-D_0 gap is roughly constant at around 20 kcal/mol. When the system reaches the "roaming region", this gap drops to ~13 kcal/mol and remains there until reaction occurs (to O + NO_2 in this case) and the surfaces become asymptotically degenerate. This clearly highlights the interaction between D_0 and D_1 in the roaming region, suggesting the ease in which D_1 may be accessed from the ground state there.

The final piece of evidence in support of this picture is the branching for dissociation on D_0 and D_1, both in that it strongly favors D_0 dissociation and is insensitive to the nature of the excitation even after a 0.7 μs delay. Although the present results are not yet definitive, in the future, with coupled D_1 and D_0 surfaces, we should be able to probe these questions theoretically by comparing the D_1 and D_0 branching starting from either surface initially. This effort is underway.

AUTHOR INFORMATION

Corresponding Author

*E-mail: asuits@wayne.edu. Phone: +1 313 577-9008.

Notes

The authors declare no competing financial interest.

ACKNOWLEDGMENTS

A.G.S. acknowledges the Army Research Office Award Number W911NF-11-10393 for financial support, and J.M.B. acknowledges the Army Research Office Award Number (W911NF-14-1-020) for financial support. B.F. acknowledges the National Natural Science Foundation of China (Grant No. 21303197) and the Chinese Academy of Sciences. A.G.S. acknowledges valuable discussions with S. North, J. F. Stanton, and T. J. Martinez.

REFERENCES

(1) Cramaros, F.; Johnston, H. S. Infrared Absorption by Symmetrical NO_3 Free Radical in Gas Phase. *J. Chem. Phys.* **1965**, *43*, 727−730.

(2) Magnotta, F.; Johnston, H. S. Photodissociation Quantum Yields for the NO_3 Free-Radical. *Geophys. Res. Lett.* **1980**, *7*, 769−772.
(3) Eisfeld, W.; Morokuma, K. Ab Initio Investigation of the Vertical and Adiabatic Excitation Spectrum of NO_3. *J. Chem. Phys.* **2001**, *114*, 9430−9440.
(4) Stanton, J. F. On the Vibronic Level Structure in the NO_3 Radical. I. The Ground Electronic State. *J. Chem. Phys.* **2007**, *126*, 134309.
(5) Stanton, J. F. On the Vibronic Level Structure in the NO_3 Radical: II. Adiabatic Calculation of the Infrared Spectrum. *Mol. Phys.* **2009**, *107*, 1059−1075.
(6) Hirota, E.; Kawaguchi, K.; Ishiwata, T.; Tanaka, I. Vibronic Interactions in the NO_3 Radical. *J. Chem. Phys.* **1991**, *95*, 771−775.
(7) Davis, H. F.; Kim, B. S.; Johnston, H. S.; Lee, Y. T. Dissociation Energy and Photochemistry of NO_3. *J. Phys. Chem.* **1993**, *97*, 2172−2180.
(8) Mikhaylichenko, K.; Riehn, C.; Valachovic, L.; Sanov, A.; Wittig, C. Unimolecular Decomposition of NO_3: The NO + O_2 Threshold Regime. *J. Chem. Phys.* **1996**, *105*, 6807−6817.
(9) Johnston, H. S.; Davis, H. F.; Lee, Y. T. NO_3 Photolysis Product Channels: Quantum Yields from Observed Energy Thresholds. *J. Phys. Chem.* **1996**, *100*, 4713−4723.
(10) Cantrell, C. A.; Stockwell, W. R.; Anderson, L. G.; Busarow, K. L.; Perner, D.; Schmeltekopf, A.; Calvert, J. G.; Johnston, H. S. Kinetic-Study of the NO_3-CH_2O Reaction and Its Possible Role in Nighttime Tropospheric Chemistry. *J. Phys. Chem.* **1985**, *89*, 139−146.
(11) Grubb, M. P.; Warter, M. L.; Suits, A. G.; North, S. W. Evidence of Roaming Dynamics and Multiple Channels for Molecular Elimination in NO_3 Photolysis. *J. Phys. Chem. Lett.* **2010**, *1*, 2455−2458.
(12) Grubb, M. P.; Warter, M. L.; Xiao, H. Y.; Maeda, S.; Morokuma, K.; North, S. W. No Straight Path: Roaming in Both Ground- and Excited-State Photolytic Channels of NO_3 → NO + O_2. *Science* **2012**, *335*, 1075−1078.
(13) Grubb, M. P.; Warter, M. L.; Johnson, K. M.; North, S. W. Ion Imaging Study of NO_3 Radical Photodissociation Dynamics: Characterization of Multiple Reaction Pathways. *J. Phys. Chem. A* **2011**, *115*, 3218−3226.
(14) Townsend, D.; Lahankar, S. A.; Lee, S. K.; Chambreau, S. D.; Suits, A. G.; Zhang, X.; Rheinecker, J.; Harding, L. B.; Bowman, J. M. The Roaming Atom: Straying from the Reaction Path in Formaldehyde Decomposition. *Science* **2004**, *306*, 1158−1161.
(15) Suits, A. G. Roaming Atoms and Radicals: A New Mechanism in Molecular Dissociation. *Acc. Chem. Res.* **2008**, *41*, 873−881.
(16) Bowman, J. M.; Shepler, B. C. Roaming Radicals. *Annu. Rev. Phys. Chem.* **2011**, *62*, 531−553.
(17) Bowman, J. M. Topical Review: Roaming. *Mol. Phys.* **2014**, 2516−2528.
(18) Xiao, H. Y.; Maeda, S.; Morokuma, K. Excited-State Roaming Dynamics in Photolysis of a Nitrate Radical. *J. Phys. Chem. Lett.* **2011**, *2*, 934−938.
(19) Grubb, M. P.; Warter, M. L.; North, S. W. Stereodynamics of Multistate Roaming. *Phys. Chem. Chem. Phys.* **2012**, *14*, 6733−6740.
(20) Fu, B. N.; Bowman, J. M.; Xiao, H. Y.; Maeda, S.; Morokuma, K. Quasiclassical Trajectory Studies of the Photodissociation Dynamics of NO_3 from the D_0 and D_1 Potential Energy Surfaces. *J. Chem. Theory Comput.* **2013**, *9*, 893−900.
(21) Luque, J.; Crosley, D. R. LIFBASE: Database and Spectral Simulation Program, version 1.5; *SRI International Report MP 99-009*; 1999.
(22) Fu, B. N.; Han, Y. C.; Bowman, J. M.; Leonori, F.; Balucani, N.; Angelucci, L.; Occhiogrosso, A.; Petrucci, R.; Casavecchia, P. Experimental and Theoretical Studies of the O(^{3}P) + C_2H_4 Reaction Dynamics: Collision Energy Dependence of Branching Ratios and Extent of Intersystem Crossing. *J. Chem. Phys.* **2012**, *137*, 22A532.
(23) Townsend, D.; Minitti, M. P.; Suits, A. G. Direct Current Slice Imaging. *Rev. Sci. Instrum.* **2003**, *74*, 2530−2539.
(24) Xiao, H. Y.; Maeda, S.; Morokuma, K. Global Ab Initio Potential Energy Surfaces for Low-Lying Doublet States of NO_3. *J. Chem. Theory Comput.* **2012**, *8*, 2600−2605.
(25) Earls, L. T. Intensities in $^2\Pi-^2\Sigma$ Transitions in Diatomic Molecules. *Phys. Rev.* **1935**, *48*, 423−424.
(26) Douglas, A. E. Anomalously Long Radiative Lifetimes of Molecular Excited States. *J. Chem. Phys.* **1966**, *45*, 1007−1015.
(27) Carter, R. T.; Schmidt, K. F.; Bitto, H.; Huber, J. R. A High-Resolution Study of the NO_3 Radical Produced in a Supersonic Jet. *Chem. Phys. Lett.* **1996**, *257*, 297−302.
(28) Nelson, H. H.; Pasternack, L.; Mcdonald, J. R. Excited-State Dynamics of NO_3. *J. Chem. Phys.* **1983**, *79*, 4279−4284.
(29) Martinez, T. J. Ab Initio Molecular Dynamics Around a Conical Intersection: Li(2p) + H_2. *Chem. Phys. Lett.* **1997**, *272*, 139−147.